

Electrical characteristics of HfO₂/La₂O₃/HfO₂ films deposited by ECR-ALD

Woong-Sun Kim, Byung-Woo Kang and Jong-Wan Park*

Thin Film Laboratory, Department of Materials Science and Engineering, Hanyang University, Seoul 133-791, Korea

In this study, we investigated the electrical characteristics of HfO₂/La₂O₃/HfO₂ capacitor (HLH capacitor) films. Lanthanum oxide (La₂O₃) and hafnium oxide (HfO₂) films were deposited by an electron cyclotron resonance plasma-enhanced atomic layer deposition method (ECR-ALD). Tris(isopropyl-cyclopentadienyl)lanthanum (La(iPrCp)₃) and tetrakis(ethylmethylamino)hafnium (TEMAHf) were utilized as the lanthanum and hafnium precursors, respectively. The leakage current of the HLH capacitor with 2/10/2 nm layers was about 2.20×10^{-10} A/cm² at 1 MV/cm and the dielectric constant of the film was 20.2. Based on leakage current mechanism research, the dominant conduction mechanism of the HLH capacitor is Poole-Frenkel (P-F) and space-charge-limited current (SCLC) conduction.

Key words: hafnium oxide, lanthanum oxide, capacitor, high-k oxide.

Introduction

As the minimum feature size of a dynamic random access memory (DRAM) shrinks, high-k dielectric materials such as Ta₂O₅, Al₂O₃, and HfO₂ have been investigated for use as DRAM capacitors. However, Ta₂O₅ has problems with reliability issues caused by a leakage current [1], while Al₂O₃ shows too low a dielectric constant for the next generation capacitors. HfO₂ is expected to have better characteristics than Ta₂O₅ and Al₂O₃ as it has a larger bandgap than Ta₂O₅ [2] and a higher dielectric constant than Al₂O₃. Furthermore, by incorporating stacked structures which have a higher conduction band offset (CBO) than HfO₂, a lower leakage current is expected.

Among the possible stack materials to be incorporated, La₂O₃ appears promising not only because of its high permittivity (K~25), but also because of its large band gap (6.4 eV). Moreover, the CBO of La₂O₃ is 2.3 eV, which is much higher than that of HfO₂ [3]. Furthermore, La₂O₃ reacts with water vapor to form lanthanum hydroxide. To overcome these limitations, we evaluated the performance of a new dielectric film stack, HfO₂/La₂O₃/HfO₂ (hereafter referred to as an HLH capacitor).

Atomic layer deposition (ALD) is an excellent deposition method due to its superb process controllability, even for extremely low thickness high-k dielectrics [4-6]. ALD is a thin-film deposition technique in which the precursors, reactants, and purge gas are supplied separately to the substrate. It can provide good film uniformity as well as low temperature deposition. Due to the nature of the self-limiting reaction, it is possible to achieve excellent step coverage and accurately control the film thickness [7]. Thus we used the ALD method

to grow the HLH capacitor.

In this paper, we deposited alternating layers of La₂O₃ and HfO₂ to form HLH stacked films. Electron cyclotron resonance plasma-enhanced atomic layer deposition (ECR-ALD) was used to deposit the HLH films. When microwave energy is delivered to electrons with a resonance frequency less than that of the static magnetic field, an ECR plasma is generated. We used an ECR plasma in our study because it is produced as a high density plasma under low pressure, and substrate damage due to ion collisions is not of major concern because no electrode is present. Tris(isopropyl-cyclopentadienyl)lanthanum (La(iPrCp)₃) (as the lanthanum precursor), tetrakis(ethylmethylamino)hafnium (TEMAHf) (as the hafnium precursor), and an O₂ plasma (as an oxygen source) were utilized. Current-voltage (I-V) and capacitance-voltage (C-V) measurements were employed to investigate the electrical properties of the materials formed.

Experimental and Procedure

HLH stacks were deposited on n-type Si substrates using ECR-ALD with La(iPrCp)₃ and TEMAHf as the lanthanum and hafnium precursors, respectively, and an O₂ plasma as an oxygen source. To obtain a hydrogen-terminated surface, the Si substrates were dipped in a diluted HF (HF : H₂O = 1 : 100) solution and then rinsed in de-ionized water. The temperatures of the La(iPrCp)₃ and the TEMAHf were maintained at 150 °C and 60 °C, respectively. The La source was carried by Ar gas at 20 sccm, while the Hf source was injected without a carrier gas. The ECR plasma power was 500 W and the deposition temperature was varied from 150 °C to 350 °C. The injection times of the La source, Hf source, and O₂ plasma were fixed at 5 s, 5 s, and 10 s, respectively.

The total cycle consisted of three steps to deposit the La₂O₃ and HfO₂ films separately. The first and third step sequences consisted of TEMAHf (5 s)/Ar (10 s)/O₂ (10 s)/

*Corresponding author:
Tel : +82-2-2220-0386
Fax: +82-2-2298-2850
E-mail: jwpark@hanyang.ac.kr

Ar (10 s), while the second step was $\text{La}(\text{iPrCp})_3$ (5 s)/ Ar (10 s)/ O_2 (10 s)/Ar (10 s). The HLH stacks with alternating La_2O_3 and HfO_2 layers were deposited repeatedly. To control the thickness of the La_2O_3 and HfO_2 layers, the number of repeated cycles of La_2O_3 and HfO_2 was varied.

To investigate the electrical properties of the HLH films, Al/HLH/n-Si metal-insulator-semiconductor capacitor (MISCAP) structures were prepared using a shadow mask and evaporator. The capacitance-voltage characteristics were measured using a HP4284A. Leakage current measurements were taken using a HP4145B semiconductor parameter. The equivalent oxide thickness (EOT) was calculated using the CVC program. The film thickness according to the number of ALD cycles was measured using an ellipsometer (Rudolph AutoEL-II).

Results and Discussion

Self-limiting ALD reactions are typically observed in the 200–400 °C range. Fig. 1 shows the dependence of the La_2O_3 and HfO_2 film growth rates on the deposition temperature between 150–350 °C. The growth rates of HfO_2 and La_2O_3 were saturated and independent of deposition temperature above 200 °C and 300 °C, respectively. In this region, one can clearly see the ALD window in which the self-limiting mechanism occurs. The growth rates were measured by varying the injection time of the $\text{La}(\text{iPrCp})_3$ and TEMAHf sources to confirm the self-limiting nature of the film growth reaction. The growth rate of the film was well saturated 2 s after the injection of the $\text{La}(\text{iPrCp})_3$ and 3 s after the injection of TEMAHf sources, respectively, as shown in the inset figure.

Leakage current measurements for different samples are compared in Fig. 2. As the total film thickness increased, the leakage current property improved. The lowest leakage current density was observed for the 2/10/2 nm HLH stack film and this value is much lower than previous reports of 15 nm- HfO_2 and 50 nm- La_2O_3 deposited by ALD [8–9]. Fig. 2 also shows the dielectric constant of the stacked

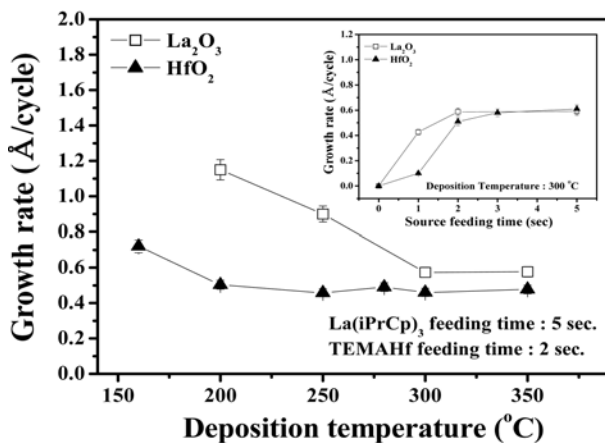


Fig. 1. Dependence of growth rate on deposition temperature. The inset figure shows film thickness as a function of the injection time of the $\text{La}(\text{iPrCp})_3$ and TEMAHf sources.

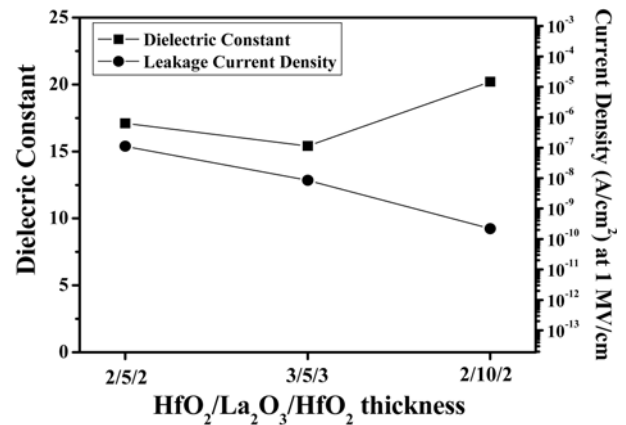


Fig. 2. Dielectric constant and leakage current density of HLH capacitors.

capacitors. As seen in the figure, the dielectric constant decreases as the HfO_2 thickness increases. The exact values of dielectric constants were 17.1, 15.4, and 20.2 for the 2/5/2, 3/5/3, and 2/10/2 nm HLH capacitors, respectively. It has been reported that lanthanum oxide forms hydride or hydroxide materials after absorbing moisture which have much lower dielectric constants than the original material [10]. However, the dielectric constants in this paper were larger than the values of La-silicate from the La-hydroxide phase. Therefore, thin HfO_2 film seems to effectively passivate La_2O_3 from the ambient.

As mentioned in a previous report, when evaluating promising capacitor materials, it is important to consider the trade-off between a high dielectric constant for high capacitor density and a wide bandgap for low capacitor leakage [11]. The HLH stack capacitor is very attractive as a capacitor material, because La_2O_3 lowered the leakage current density due to its large conduction band offset without lowering the dielectric constant (Fig. 2). Moreover, according to recent reports, La_2O_3 insertion at the HfO_2/Si interface results in higher capacitance [12–13].

Fig. 3 shows the leakage current density-voltage charac-

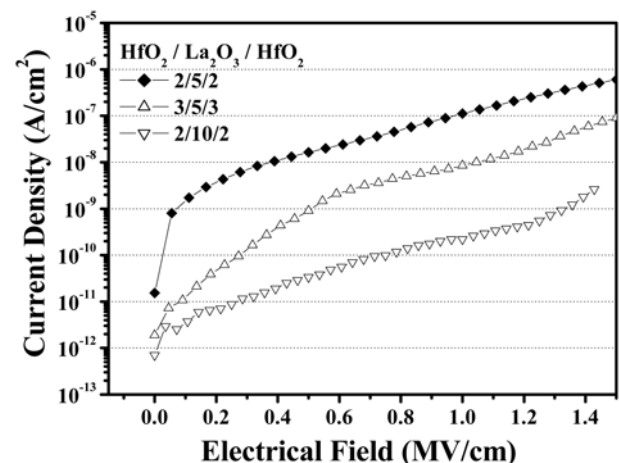


Fig. 3. Characteristics of current density versus electrical field for HLH capacitors.

teristics of HLH stack capacitors of different thicknesses. The measured area is $3.14 \times 10^{-4} \text{ cm}^2$ for all of the samples. The leakage current densities for the HLH capacitor with 2/5/2, 3/5/3, and 2/10/2 nm are 1.12×10^{-7} , 8.53×10^{-9} , and $2.20 \times 10^{-10} \text{ A/cm}^2$ at 1 MV/cm, respectively.

The leakage current characteristics of a HLH capacitor with 2/10/2 nm as a function of test temperature are shown in Fig. 4. The leakage currents were measured from 300 to 400 K. The test at a temperature of 300 K (Fig. 4(a)) showed that the main conduction mechanism is space-charge-limited current (SCLC). Numerous attempts have made to interpret the current behavior of La_2O_3 films within the frame of SCLC [14-16]. SCLC results from carriers injected into an insulator where no compensating charge is present. The current characteristics equations of SCLC are as follows:

$$J_{Child} = \frac{9\epsilon_i \mu V^2}{8d^3} \quad (1)$$

$$J_{Ohm} = qn_o \mu \frac{V}{d} \quad (2)$$

where ϵ_i is the insulator permittivity, μ is the mobility in the insulator, d is the insulator thickness, q is the electronic charge, n_o is the concentration of free charge carriers in thermal equilibrium, and V is the applied voltage.

As shown in Fig. 5, the current characteristics in the log

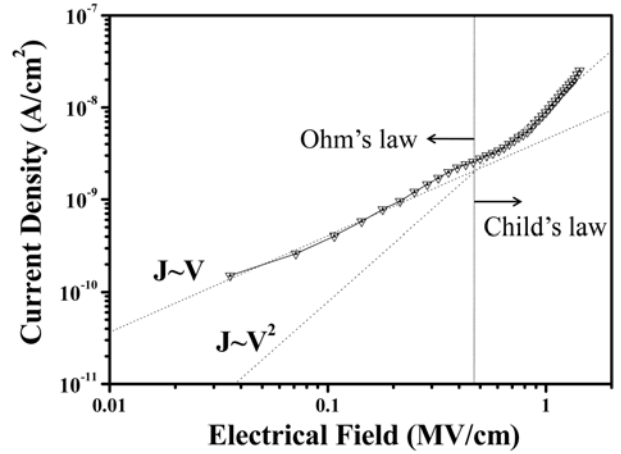


Fig. 5. Logarithm of the current density plotted as a function of the logarithm of the applied voltage of the HLH capacitor with 2/10/2 nm at a temperature of 300 K.

J-log V plane are divided by two limited curves, namely, Ohm's law ($J \propto V$) and Child's law ($J \propto V^2$). According to SCLC theory, the current-voltage characteristics should initially be ohmic ($J \sim V$), as shown in Fig. 5 at low applied voltage. After that, the current is proportional to the square of the applied voltage as shown in equation (1). The transition from Ohm's law to Child's law is observed around 0.4 V. Figs. 4(a) and 5 show that the current characteristics for a HLH capacitor with 2/10/2 nm at 300 K can be

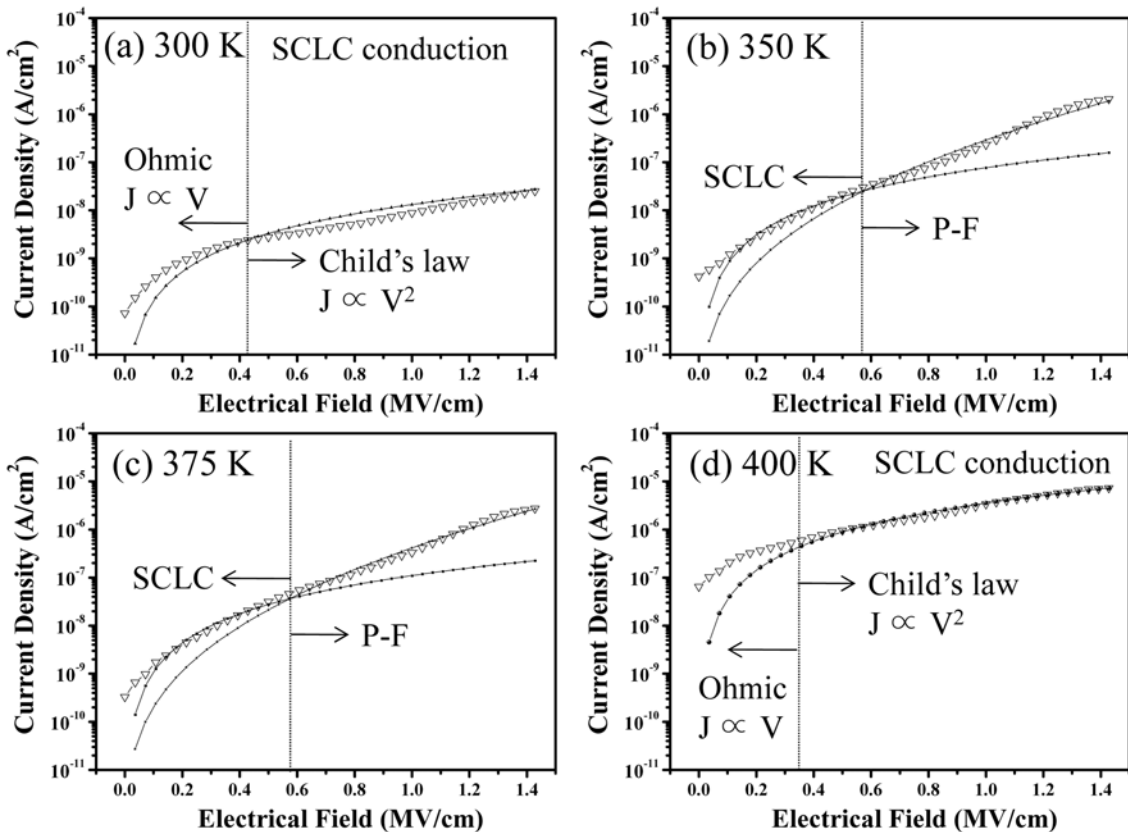


Fig. 4. Current characteristics of HLH capacitor with 2/10/2 nm at temperatures from 300 to 400 K.

fitted to SCLC behavior.

For a test at temperatures of 350 K and 375 K (Figs. 4(b), (c)), current characteristics can be fitted to an SCLC mechanism at a low electrical field and Poole-Frenkel (P-F) conduction at a higher field. The transition from SCLC to P-F is observed around 0.6 V. The P-F conduction is due to emission of trapped electrons into the conduction band. In high dielectric constant thin films such as HfO_2 and ZrO_2 , P-F conduction behavior has frequently been observed due to the high density of traps [17-19]. The following equation (3) expresses the conduction process in HfO_2 , where the P-F is considered to be the main conduction mechanism due to bulk defects at 350 K and 375 K:

$$J \propto E_i \exp\left[\frac{-q(\Phi_B - \sqrt{qE_i/\pi\epsilon_i})}{kT}\right] \quad (3)$$

where Φ_B is the barrier height and E_i is the electric field in the insulator.

A very strong increase in leakage is observed when raising the temperature up to 400 K. For a test at temperature 400 K (Fig. 4(d)), current characteristics can be fitted to an SCLC mechanism as well. The current characteristic is very similar to that seen at 300 K. However, the transition from Ohm's law to Child's law is observed below 0.4 V because the onset voltage of the SCLC conduction decreases with increasing temperature [15].

Conclusions

We have investigated the electrical properties of HLH films with various film thicknesses. The dielectric constant of the HLH capacitors were 17.1, 15.4, and 20.2 for the 2/5/2, 3/5/3, and 2/10/2 nm thicknesses, respectively. The temperature dependence of leakage current was investigated to determine the electrical conduction mechanisms of the HLH capacitor. The leakage current of the HLH capacitor with a thickness of 2/10/2 nm was about 2.20×10^{-10} A/cm² at 1 MV/cm. Previous report showed that P-F and SCLC mechanism are the main conduction mechanisms for metal/ La_2O_3 /n-Si insulators [15]. In this study, P-F and SCLC conduction were studied for the HLH capacitor.

Experimental results showed that the main conduction mechanisms were consistent with P-F and SCLC.

References

1. B.C. Lai and J.Y. Lee, *J. Electrochem. Soc.* 146 (1999) 266-269.
2. J. Robertson, *J. Vac. Sci. Technol.* B18 (2000) 1785-1791.
3. T. Hattori, T. Yoshida, T. Shiraishi, K. Takahashi, H. Nohira, S. Joumori, K. Nakajima, M. Suzuki, K. Kimura, I. Kashiwagi, C. Ohshima, S. Ohmi and H. Iwai, *Microelectron. Eng.* 72, (2004) 283-287.
4. T. Delage, C. Champeaux, A. Catherinot, J.F. Seaux, V. Mdrangeas and D. Cros, *Thin Solid Films* 453 (2004) 279-284.
5. A.R. Teren, R. Thomas, J. He and P. Ehrhart, *Thin Solid Films* 478 (2005) 206-217.
6. H.Y. Yua, M.F. Li and D.L. Kwong, *Thin Solid Films* 462 (2004) 110-113.
7. B.S. Lim, A. Rahtu and R.G. Gordon, *Nat. Mater.* 2 (2003) 749-754.
8. N.K. Park, D.K. Kang, B.H. Kim, S.J. Jo and J.S. Ha, *Appl. Surf. Sci.* 252 (2006) 8506-8509.
9. H.B. Park, M.J. Cho, J.H. Park, S.W. Lee, C.S. Hwang, J.P. Kim, J.H. Lee, N.I. Lee, H.K. Kang, J.C. Lee and S.J. Oh, *J. Appl. Phys.* 94 (2003) 3641-3647.
10. K. Kakushima, K. Tsutsui, S.I. Ohmi, P. Ahmet, V.R. Rao and H. Iwai, *Topics Appl. Physics* 106 (2007) 345-365.
11. E. Gerritsen, N. Emonet, C. Caillat, N. Jourdan, M. Piazza, D. Fraboulet, B. Boeck, A. Berthelot, S. Smith and P. Mazoyer, *Solid State Electron.* 49 (2005) 1767-1775.
12. K. Kakushima, K. Okamoto, M. Adachi, K. Tachi, P. Ahmet, K. Tsutsui, N. Sugii, T. Hattori and H. Iwai, *Solid State Electron.* 52 (2008) 1280-1284.
13. K. Kakushima, K. Okamoto, M. Adachi, K. Tachi, J. Song, S. Sato, T. Kawanago, P. Ahmet, K. Tsutsui, N. Sugii, T. Hattori and H. Iwai, *Appl. Surf. Sci.* 254 (2008) 6106-6108.
14. Y. Kim, K. Miyauchi, S. Ohmi, K. Tsutsui and H. Iwai, *Microelectron J.* 36 (2005) 41-49.
15. F. Chiu, H. Chou and J.Y. Lee, *J. Appl. Phys.*, 97 (2005) 103503-1-103503-5.
16. Y. Kim, S. Ohmi, K. Tsutsui, H. Iwai, *Solid State Electron.* 49 (2005) 825-833.
17. W.J. Zhu, T.P. Ma, T. Tamagawa, J. Kim and Y. Di, *IEEE Electron Device Lett.* 23 (2002) 97-99.
18. J.P. Chang and Y.S. Lin, *Appl. Phys. Lett.* 79 (2001) 3666-3668.
19. D.S. Jeong, H.B. Park and C.S. Hwang, *Appl. Phys. Lett.* 86 (2005) 072903-1-072903-3.